machines

MDPI

Article

Feedrate Profile Shaping-Based Five-Axis CNC Feedrate Planning Method Under Machine Axis Constraints

Shaofeng Zhang [1], Qiang Ma [1], Liping Wang [2], Hongli Yang [2], Yuanshenglong Li [2], Dong Wang [2], Jingjing Cao [1], Jinfan Li [2], Yongqi Wang [3] and Weiwei He [1,*]

[1] School of Mechanical and Equipment Engineering, Hebei University of Engineering, Handan 056038, China; s23zhangshaofeng1023@hebeu.edu.cn (S.Z.); maqiang@hebeu.edu.cn (Q.M.); caojingjing@hebeu.edu.cn (J.C.)
[2] Department of Mechanical Engineering, Tsinghua University, Beijing 100084, China; lpwang@mail.tsinghua.edu.cn (L.W.); yanghl20@mails.tsinghua.edu.cn (H.Y.); lysl22@mails.tsinghua.edu.cn (Y.L.); d-wang@mail.tsinghua.edu.cn (D.W.); lijf23@mails.tsinghua.edu.cn (J.L.)
[3] School of Mechanical and Electrical Engineering, University of Electronic Science and Technology of China, Chengdu 611731, China; 202321040116@std.uestc.edu.cn
* Correspondence: heweiwei@hebeu.edu.cn

Abstract

Feedrate planning is a critical process in computer numerical control (CNC) machining, playing a key role in ensuring machining quality and improving efficiency. This paper proposes a feedrate planning method based on feedrate profile shaping to satisfy machine axis constraints, including axis velocity, acceleration, and jerk limits. First, the five-axis machining path is represented using parametric curves. By combining the geometric characteristics of the path with machine axis velocity constraints, the upper bound of the feedrate under static constraints is derived. On this basis, machine axis acceleration and jerk constraints are further incorporated to establish feedrate planning criteria, thereby obtaining a distribution of feasible points that satisfies dynamic constraints. Then, a feedrate curve is generated using a profile shaping strategy based on the feasible point distribution, and further optimized through a corner shaping method. As a result, the planned feedrate strictly satisfies machine axis constraints along the entire tool path while ensuring continuity and smoothness of the feedrate profile. Finally, the effectiveness and reliability of the proposed method are validated through simulations of the parametric curve and experimental machining of an impeller blade.

Keywords: feedrate profile shaping; machine axis constraints; feedrate planning; CNC

Check for updates

Academic Editor: Gianni Campatelli

Received: 12 January 2026
Revised: 2 February 2026
Accepted: 3 February 2026
Published: 4 February 2026

Copyright: © 2026 by the authors. Licensee MDPI, Basel, Switzerland. This article is an open access article distributed under the terms and conditions of the Creative Commons Attribution (CC BY) license.

1. Introduction

With the increasingly stringent requirements for both accuracy and efficiency in complex surface machining in high-end manufacturing fields such as aerospace and automotive mold production, high-speed computer numerical control (CNC) machining has become a core driving force of modern manufacturing. During high-speed machining, parametric curves—represented by non-uniform rational B-splines (NURBS)—have been widely adopted for toolpath representation due to their ability to describe arbitrary curves in a unified mathematical form and their excellent geometric continuity, thereby serving as a fundamental carrier of parametric interpolation techniques [1–5]. As a key component of CNC machining, feedrate planning directly determines machining efficiency and quality [6]. Current feedrate planning along parametric paths faces several challenges. First, coordinating static and dynamic constraints remains a major challenge. Static constraints

include geometric constraints such as chord error, normal acceleration, and normal jerk, as well as machine axis velocity limits, while dynamic constraints involve machine axis acceleration and jerk limits together with the overall machine acceleration constraint. The feedrate along a parametric path must simultaneously satisfy both categories of constraints. When these constraints are violated, feedrate overruns or overload of the machine drive system may occur, adversely affecting machining quality and operational stability [7]. Second, feedrate-sensitive regions (FSRs) often exist in complex toolpaths, where feedrate reduction is usually required to maintain machining stability [8]. Although traditional constant-speed transition strategies are computationally simple, they significantly reduce machining efficiency, especially when multiple sensitive regions occur consecutively, leading to more pronounced efficiency losses. In addition, the feedrate profile should maintain sufficient smoothness and rationality to ensure machining quality and accuracy [9]. This study defines feedrate constraint modeling and feedrate profile generation as the two key stages of five-axis CNC feedrate planning, and investigates the problem by focusing on these two stages.

Achieving rational feedrate planning under the combined effects of multiple constraints is essential for ensuring machining quality. Zhao et al. [10] introduced accuracy constraints for two-dimensional and three-dimensional trajectories, respectively, to achieve feedrate optimization in high-precision CNC machining. Guo et al. [11] ensured the machining accuracy of NURBS curves by incorporating chord error and normal acceleration constraints. Zhang et al. [12] investigated the optimal feedrate planning problem for three-axis CNC machines along curved toolpaths under axis acceleration and jerk limits, as well as tangential velocity constraints. Xavier et al. [13] computed the maximum achievable feedrate based on the kinematic constraints of individual drives and iteratively smoothed five-axis toolpaths to increase the actual feedrate; however, the influence of geometric constraints on feedrate was neglected. Sang et al. [14] considered single-axis kinematic constraints, but in terms of geometric constraints, only those arising from path deviations were taken into account, and a constant feedrate was applied in difficult-to-machine regions to maintain process stability. Ma et al. [15] imposed constraints on joint-space velocity, acceleration, and jerk, as well as Cartesian-space chord error, to achieve feedrate planning for five-axis parametric toolpaths. Tang et al. [16] considered kinematic constraints to ensure that axis velocity, acceleration, and jerk remain within user-defined limits. Huang et al. [17] employed a velocity segmentation optimization algorithm under jerk constraints to dynamically optimize speeds exceeding servo limits, ensuring they remain within allowable ranges; however, geometric constraints of the machining path were not considered. In summary, some studies on feedrate planning only consider partial static constraints and completely ignore machine axis constraints. Other studies take machine kinematic constraints into account but lack comprehensive consideration of path geometric constraints. Therefore, feedrate planning that fully accounts for the geometric constraints of parametric paths while simultaneously incorporating machine axis drive constraints for multi-constraint coordinated optimization remains an area requiring further investigation.

In the machining of complex trajectories, high geometric curvature often leads to the formation of FSRs in the feedrate profile. Within these regions, excessively high feedrates can cause the drive axes to exceed kinematic limits, resulting in contour errors and machine vibrations. Therefore, rational feedrate planning based on FSRs not only improves the surface quality of the machined trajectory but also effectively suppresses machine vibrations and prevents drive overload, thereby significantly enhancing the stability and robustness of the machining process. Existing studies have focused on feedrate planning for high-curvature trajectory segments and FSRs. Huang and Wang [18,19] divided NURBS toolpaths into multiple sub-curves based on points of minimum curvature radius (PMR) to

enable independent feedrate scheduling for each sub-curve, improving speed adaptability in high-curvature regions. However, this approach is prone to feedrate overruns at PMR locations, potentially affecting machining accuracy. Jia et al. [20] introduced the concept of FSRs and developed a NURBS interpolation method that maintains a constant feedrate under both drive and contour error constraints. Ma et al. [21] categorized feedrate into sensitive and non-sensitive regions, applying a constant feedrate in sensitive regions and a smoothly transitioning feedrate in non-sensitive regions, thereby balancing motion stability and efficiency. Nie et al. [22] proposed a two-stage scanning method for FSRs and applied different feedrate scheduling strategies within these regions to ensure real-time performance and machining stability. Although existing studies generally reduce feedrates in FSRs to ensure system stability, overly conservative feedrate profile generation strategies can significantly reduce machining efficiency. Therefore, generating an optimal feedrate profile based on FSRs has become a key issue for further improving machining efficiency.

Based on the above analysis, this paper proposes a novel feedrate planning method based on feedrate profile shaping (FPS). The overall framework of the method is illustrated in Figure 1. First, the allowable feedrate is calculated based on static constraints. FSRs are then identified through a combination of global coarse scanning and local fine scanning, determining the start points, end points, extremum points, and their corresponding feedrates for each FSR. Next, feedrate profile shaping criteria are established according to dynamic constraints, converting them into limits on the tangent slope of the feedrate curve, and feasible points satisfying these slope limits are identified within the sensitive regions. Subsequently, the feedrate profile is shaped based on the feasible points within the sensitive regions and extended to the non-sensitive regions. Finally, corner shaping is applied to the initially shaped feedrate curve under jerk constraints, resulting in a smooth feedrate profile that satisfies all constraints. The innovative contributions of this method are as follows: in terms of feedrate constraints, it simultaneously considers the geometric characteristics of the parametric path and the drive constraints of the machine axes to establish feedrate planning criteria under multiple constraints; in terms of feedrate planning, a feedrate profile shaping strategy is applied to adjust the feedrate curve within FSRs, and a corner shaping strategy is further employed to optimize the feedrate curve, ensuring both machining efficiency and process stability.

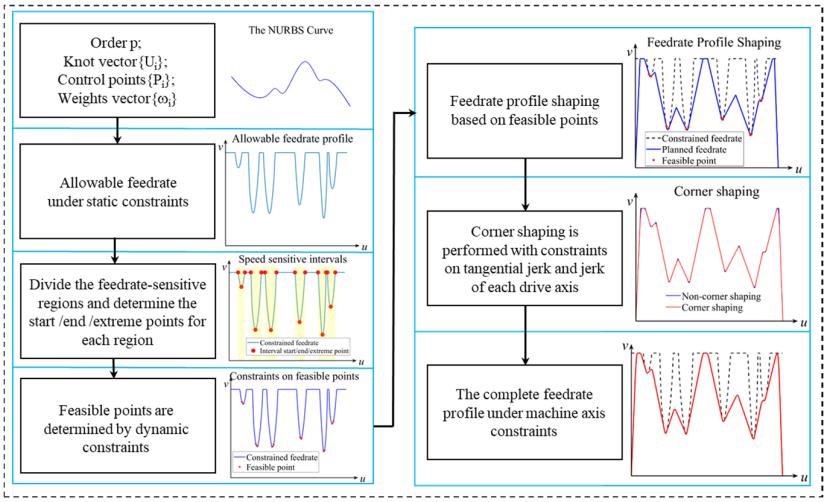


Figure 1. Flowchart of the proposed feedrate planning method.

The remainder of this paper is organized as follows: Section 2 presents the establishment of feedrate constraints under static conditions. Section 3 details the specific procedures

of the FPS method. Section 4 validates the feasibility of the proposed method through simulations and experiments. Finally, Section 5 provides a summary of the work.

2. Feedrate Constraints Under Static Conditions

2.1. Parametric Path Representation

In CNC machining, representing the toolpath using a parametric path focuses on accurately describing complex contours through a unified mathematical model, while facilitating coordinated control of interpolation accuracy and feedrate by the CNC system to meet the requirements of high-precision and high-stability machining. NURBS curves, due to their high-precision representation of complex geometries and flexible control characteristics, have become a typical form of parametric paths and are now widely used in the fields of computer-aided design (CAD), computer-aided manufacturing (CAM), and computer-aided engineering (CAE). For a given NURBS path curve $\boldsymbol{P}(u)$, it can be expressed in the following form [8]:

$$\boldsymbol{P}(u) = \sum_{i=0}^{m} N_{i,k}(u)\omega_i \boldsymbol{p}_i / \sum_{i=0}^{m} N_{i,k}(u)\omega_i \;\; u \in [0,1] \tag{1}$$

where $\boldsymbol{p}_i$ denotes the control points, ω_i denotes the weights, and $N_{i,k}(u)$ denotes the k-th order B-spline basis functions defined over the knot vector. The B-spline basis functions $N_{i,k}(u)$ are computed as follows [8]:

$$N_{i,0}(u) = \begin{cases} 1, & \text{if} u_i \le u \le u_{i+1} \\ 0, & \text{otherwise} \end{cases} \tag{2}$$

$$N_{i,k}(u) = \frac{u - u_i}{u_{i+k} - u_i} N_{i,k-1}(u) + \frac{u_{i+k+1} - u}{u_{i+k+1} - u} N_{i+1,k-1}(u) \tag{3}$$

Here, the convention "0/0 = 0" is applied.

The first and second derivatives of the B-spline basis functions and the NURBS curve are given by [20]:

$$N'_{i,k}(u) = \frac{k}{u_{i+k} - u_i} N_{i,k-1}(u) - \frac{k}{u_{i+k+1} - u_{i+1}} N_{i+1,k-1}(u) \tag{4}$$

$$N''_{i,k}(u) = \frac{k}{u_{i+k} - u_i} N'_{i,k-1}(u) - \frac{k}{u_{i+k+1} - u_{i+1}} N'_{i+1,k-1}(u) \tag{5}$$

and

$$\boldsymbol{P}'(u) = \frac{\sum_{i=0}^{n} N'_{i,k}(u)\omega_i \boldsymbol{p}_i - \boldsymbol{P}(u)\sum_{i=0}^{n} N'_{i,k}(u)\omega_i}{\sum_{i=0}^{n} N_{i,k}(u)\omega_i} \tag{6}$$

$$\boldsymbol{P}''(u) = \frac{\sum_{i=0}^{n} N''_{i,k}(u)\omega_i \boldsymbol{p}_i - 2\boldsymbol{P}'(u)\sum_{i=0}^{n} N'_{i,k}(u)\omega_i - \boldsymbol{P}(u)\sum_{i=0}^{n} N''_{i,k}(u)\omega_i}{\sum_{i=0}^{n} N_{i,k}(u)\omega_i} \tag{7}$$

The curvature radius $\rho(u)$ at any point on a NURBS curve is defined as follows:

$$\rho(u) = \frac{\|P'(u)\|^3}{\|P'(u) \times P''(u)\|} \tag{8}$$

where $\|\cdot\|$ denotes the Euclidean norm, and $\times$ denotes the vector cross product.

2.2. Static Constraints

In CNC feedrate planning, constraints can be classified into two categories: static and dynamic. Static constraints are determined by the geometric features of the path, including

geometric limitations such as chord error, normal acceleration, and normal jerk, as well as the velocity limits of each machine axis. Dynamic constraints, on the other hand, are dictated by the physical drive capabilities of the machine, encompassing limits on axis velocity, acceleration, and jerk, as well as the overall machine acceleration. Both types of constraints jointly influence the feedrate planning process, and their coordination directly affects machining accuracy, efficiency, and process stability. This subsection focuses on calculating the allowable feedrate under static constraints, which determines the maximum feasible feedrate for the initial feedrate profile and provides the foundation for subsequent FPS. Dynamic constraints, which serve as criteria for FPS, will be introduced in the next section.

The allowable feedrate is determined by static constraints. The programmed feedrate is a reference value preset during CNC programming to achieve the desired toolpath motion. At each point along the curve, the allowable feedrate is subject to multiple constraints, including chord error, normal acceleration, normal jerk, and axis velocity limits. To ensure geometric accuracy and smooth motion during parametric path interpolation, the chord error must be strictly controlled within allowable limits, normal acceleration and jerk must be constrained to prevent machine vibrations, and axis velocity limits must be respected to avoid exceeding the machine's physical capabilities. Accordingly, the allowable feedrate at each point is calculated by integrating these multiple constraints comprehensively.

2.2.1. Upper Bound of Feedrate Under Chord Error Constraint

When the feedrate is v, the chord error δ on the spline curve can be calculated as [20]:

$$\delta = \rho - \sqrt{\rho^2 - \left(\frac{vT}{2}\right)^2} \tag{9}$$

where ρ is the curvature radius of the curve, calculated using Equation (8), and T is the interpolation period. Accordingly, the feedrate $v_g(u)$ under the chord error limit constraint can be obtained from the above equation as:

$$v_g(u) = \frac{2\sqrt{2\rho\delta_{\text{lim}} - \delta_{\text{lim}}^2}}{T} \tag{10}$$

where δ_{lim} denotes the prescribed maximum allowable chord error.

2.2.2. Upper Bound of Feedrate Under Normal Acceleration and Normal Jerk Constraints

When the feedrate is v, the normal acceleration along the curve can be expressed as [20]:

$$a_n = \frac{v^2}{\rho} \tag{11}$$

Therefore, the allowable feedrate $v_a(u)$ under the normal acceleration constraint is given by:

$$v_a(u) = \sqrt{\rho a_{n,\text{lim}}} \tag{12}$$

where $a_{n,\text{lim}}$ denotes the prescribed maximum allowable normal acceleration.

Here, the normal jerk is defined as the rate of change in the normal acceleration. When the feedrate is v and the curvature radius of the curve is ρ, the feedrate $v_j(u)$ under the normal jerk constraint is given by [20]:

$$v_j(u) = \sqrt[3]{\rho^2 j_{n,\text{lim}}} \tag{13}$$

where $j_{n,\text{lim}}$ denotes the prescribed maximum allowable normal jerk.

2.2.3. Upper Bound of Feedrate Under Machine Axis Velocity Limits

Constraining the feedrate based on individual machine axis velocities primarily accounts for the drive capabilities of each axis, thereby enhancing machining stability. For a fixed parameter position u on the tool tip path curve $P(u)$, the corresponding path velocity $v(u)$ can be expressed as [8]:

$$v(u(t)) = \frac{ds}{dt} = \frac{ds}{du}\frac{du}{dt} \tag{14}$$

Here, s denotes the arc length parameter of the path curve. The derivative with respect to the parameter u is given by [8]:

$$\frac{ds}{du} = \|P_u(u)\| \tag{15}$$

Then, when the feedrate is v, the velocity of each individual drive axis can be calculated as:

$$\hat{f}(u) = \frac{dM^{\wedge}(u)}{dt} = \frac{dM^{\wedge}(u)}{du}\frac{du}{ds}\frac{ds}{dt} = M_u^{\wedge}\frac{du}{ds}v(u) \tag{16}$$

where $M^{\wedge}(u)$ denotes the coordinate components of the parametric path curve along each machine axis, $\wedge = x, y, z, \alpha, \beta$.

Then, based on the axis velocity limits $\hat{f}_{\lim}(\wedge = x, y, z, \alpha, \beta)$ set according to the drive capabilities of each machine axis, the feedrate under the axis velocity limits can be derived as:

$$v_f(u) = \frac{\hat{f}_{\lim}}{M_u^{\wedge}}\frac{ds}{du} = \frac{\hat{f}_{\lim}}{M_u^{\wedge}}\|P_u(u)\| \tag{17}$$

The programmed feedrate is denoted as v_p.Based on the above analysis, the allowable feedrate $v_{\lim}(u)$ at any point on the curve can be calculated as:

$$v_{\lim}(u) = \min\left\{v_g(u), v_a(u), v_j(u), v_f(u), v_p\right\} \tag{18}$$

3. Feedrate Profile Shaping Strategy

3.1. Partitioning of FSRs

In this study, regions of the feedrate profile where the allowable feedrate falls below the programmed feedrate are defined as feedrate-sensitive regions (FSRs), with each FSR containing a single complete cycle of feedrate decrease and subsequent increase. To accurately identify such regions, a two-stage procedure consisting of global coarse scanning and local fine scanning is employed.

In the coarse scanning stage, the entire machining path is densely sampled, and the allowable feedrate at each sample point is calculated and compared with the programmed feedrate to determine whether the point belongs to an FSR. Regions where the allowable feedrate falls below the programmed feedrate are preliminarily identified as candidate FSRs, and their approximate start points, end points, and extremum points are determined. Figure 2 illustrates a schematic of the preliminarily identified FSRs obtained through coarse scanning.

In the fine scanning stage, the preliminarily identified FSRs are further refined to ensure that each FSR contains exactly one complete cycle of feedrate decrease and increase, regions containing local maxima of curvature radius must be re-partitioned using the parameters of these maximum points as boundaries, with the start and end parameters of the FSRs accordingly adjusted. Finally, each FSR is divided into a front half and a rear half based on the parameter corresponding to the minimum curvature radius within the region, preparing for subsequent FPS. As shown in Figure 3, this procedure identifies all FSRs along the entire feedrate profile.

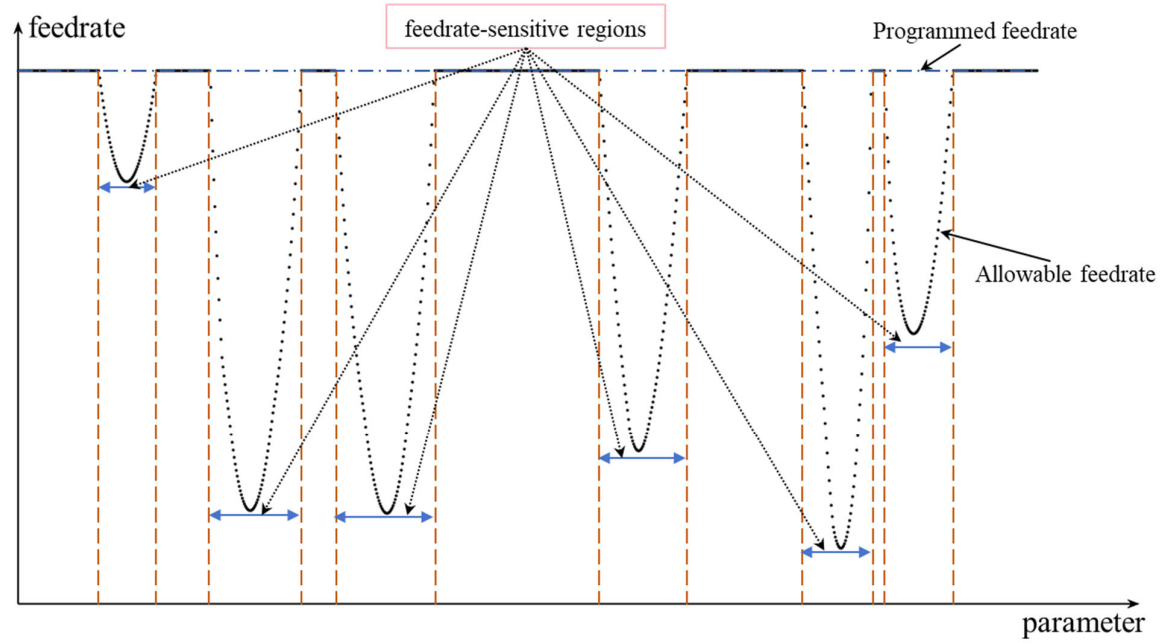


Figure 2. Schematic diagram for the preliminary determination of FSRs.

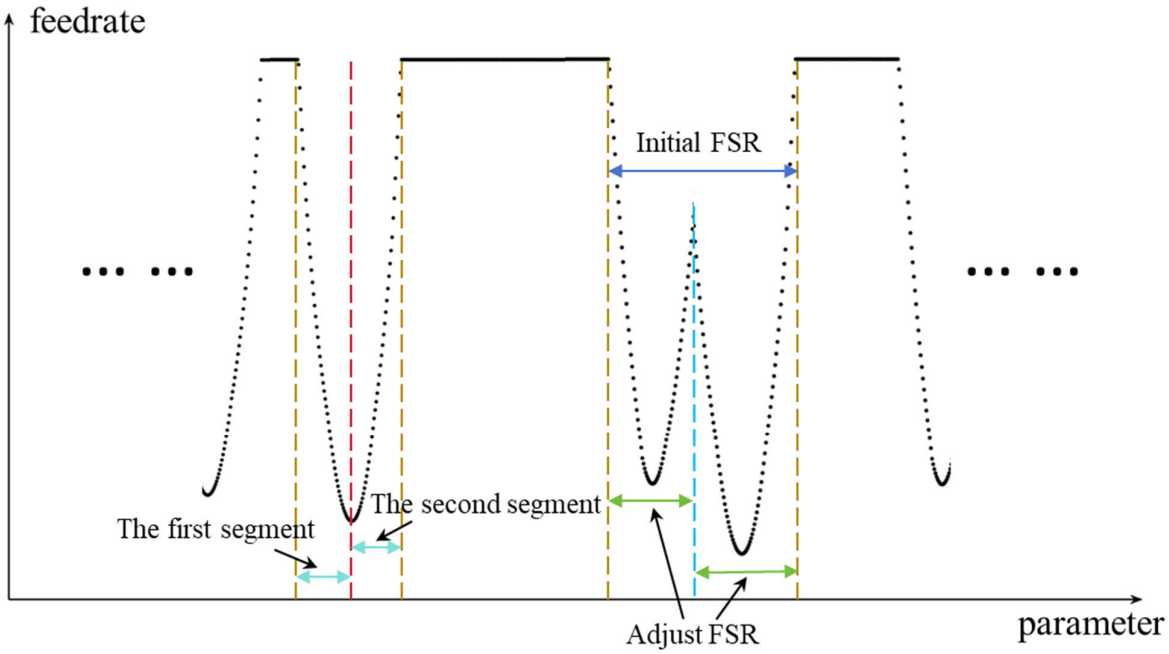


Figure 3. Adjustment and subdivision of FSR.

3.2. Feedrate Profile Shaping Within FSRs

Since the initially obtained feedrate profile only considers static constraints, it is also necessary to impose dynamic constraints, including axis acceleration and axis jerk limits as well as the overall machine acceleration limit. The absence of these dynamic constraints may result in a mismatch between the initial feedrate profile and the actual machine capabilities. By incorporating these constraints, the initial feedrate profile within FSRs is shaped to produce a feedrate curve that satisfies dynamic limitations.

According to Equation (15), a one-to-one correspondence exists between the curve parameter and the arc length, $du/ds = 1/\|P_u(u)\| = 1/k$. Here, k denotes the accumulated arc length along the machining path, representing the actual distance traveled from the start point to the current position, and is used to characterize the path length scale. The

first, second, and third derivatives of each axis trajectory with respect to time yield the expressions for the axis velocity $\hat{V}(u)$, acceleration $\hat{A}(u)$ and jerk $\hat{J}(u)$ as follows:

$$\begin{cases} \hat{V}(u) = \frac{dM^{\wedge}}{dt} = \frac{dM^{\wedge}}{du}\frac{du}{ds}\frac{ds}{dt} = M_u^{\wedge}\frac{v(u)}{k} \\ \hat{A}(u) = \frac{dV^{\wedge}}{dt} = M_{uu}^{\wedge}\left(\frac{v(u)}{k}\right)^2 + M_u^{\wedge}\frac{a(u)}{k} \\ \hat{J}(u) = \frac{dA^{\wedge}}{dt} = M_{uuu}^{\wedge}\left(\frac{v(u)}{k}\right)^3 + 3M_{uu}^{\wedge}\frac{v(u)a(u)}{k^2} + M_u^{\wedge}\frac{j(u)}{k} \end{cases} \tag{19}$$

where $\hat{} = x, y, z, \alpha, \beta$. Here, v, a, and j denote the tool tip velocity, acceleration, and jerk, respectively, and are calculated as follows:

$$a(u) = \frac{dv(u)}{dt} = \frac{dv}{du}\frac{du}{ds}\frac{ds}{dt} = v_u\frac{v(u)}{k} \tag{20}$$

$$j(u) = \frac{da(u)}{dt} = \frac{v^2}{k^2}\left[v_{uu} + \frac{{v_u}^2}{v(u)} - \frac{v_u k_u}{k}\right] \tag{21}$$

From Equations (19)–(21), the axis acceleration and jerk of the machine can be further derived as:

$$\hat{A}(u) = M_{uu}^{\wedge}\left(\frac{v(u)}{k}\right)^2 + M_u^{\wedge}\frac{v_u v(u)}{k^2} \tag{22}$$

$$\hat{J}(u) = \frac{M_{uuu}^{\wedge}}{k}v^3(u) + \frac{3M_{uuu}^{\wedge}k - M_u^{\wedge}k_u}{k^4}v^2(u)v_u + \frac{M_u^{\wedge}}{k^3}v^2(u)v_{uu} + \frac{M_u^{\wedge}}{k^3}v(u)v_u^2 \tag{23}$$

From Equation (22), it can be seen that at any point on the spline trajectory, the first and second derivatives at that point, as well as the corresponding initial velocity, are already determined. The axis accelerations are linearly related to the slope of the feedrate curve at that point, allowing the acceleration constraints at any point on the spline trajectory to be transformed into slope constraints on the corresponding points of the feedrate curve:

$$v_u \le \frac{k^2\hat{A}_{\max} - M_{uu}^{\wedge}(v(u))^2}{M_u^{\wedge}v(u)} \tag{24}$$

where $A_{\max}^{\wedge}$ denotes the acceleration limit of each axis.

In addition, limiting the overall machine acceleration in multi-axis CNC machining can improve motion smoothness and reduce machine impact. The overall machine acceleration can be calculated as follows:

$$A_{\text{total}} = A_t + A_n = v_u\frac{v(u)}{k} + \frac{v^2(u)}{\rho} \tag{25}$$

Similarly, the overall acceleration constraint at any point on the spline trajectory can be transformed into a slope constraint on the corresponding point of the feedrate curve:

$$v_u \le \frac{k\left(A_{\text{total, max}} - v^2(u)/\rho\right)}{v(u)} \tag{26}$$

where $A_{\text{total, max}}$ denotes the limit of the overall machine acceleration.

Furthermore, within each FSR, the sampling and scanning procedure described in Section 3.2 is applied. The slope of the feedrate curve at each sample point is calculated. In the front half of the region, the last parameter point that satisfies the constraints in Equations (24) and (26) is identified, while in the rear half, the first parameter point satisfying these constraints is defined as the feasible point. At each feasible point, a tangent line with the slope equal to the local feedrate derivative is drawn. In the non-sensitive regions, straight lines with constant feedrate—either the programmed feedrate or the feedrate at the local maximum of

the sensitive region—intersect with this tangent line at one point, and a line with the feedrate at the local minimum of the sensitive region intersects at another point. By traversing the entire acceleration and deceleration process in this manner, the feedrate profile after curve shaping is obtained. Figure 4 illustrates an example of FPS for a single FSR.

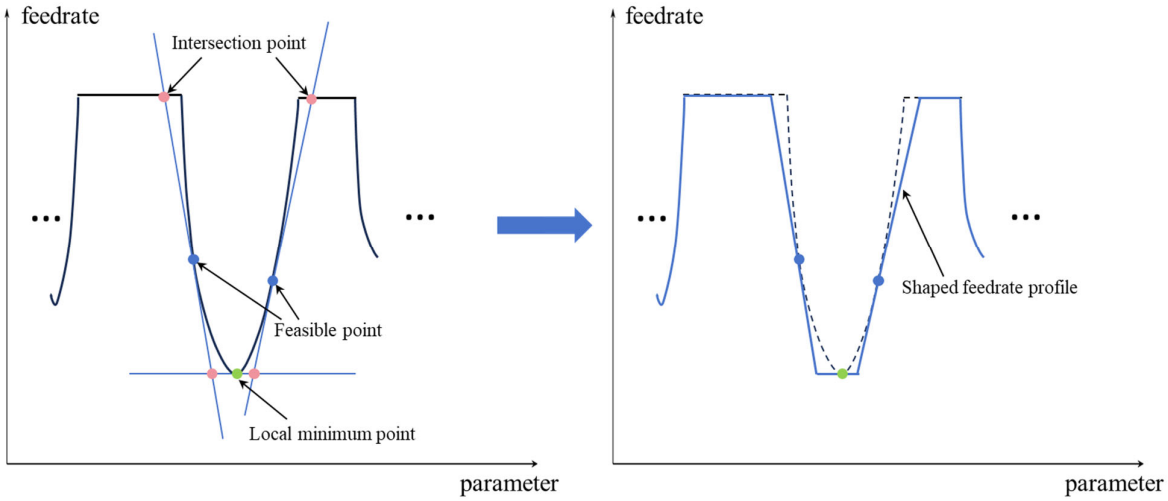


Figure 4. Example illustrating FPS.

3.3. Corner Shaping of Transition Segments in the Feedrate Profile

However, the feedrate profile obtained through the procedure in Section 3.2 may not satisfy jerk constraints, and sharp corners often appear in the acceleration/deceleration transition segments, which can negatively affect machining quality and stability. To mitigate these effects, local smoothing theory is applied to perform corner shaping in the transition segments of the feedrate profile, as shown in Figure 5. In this study, local smoothing is implemented using a quintic polynomial for the feedrate profile, which is expressed as follows:

$$V(\omega) = a_0 + a_1\omega + a_2\omega^2 + a_3\omega^3 + a_4\omega^4 + a_5\omega^5 \tag{27}$$

where $\omega = \frac{u-u_L}{h}$, $h = u_R - u_L$.

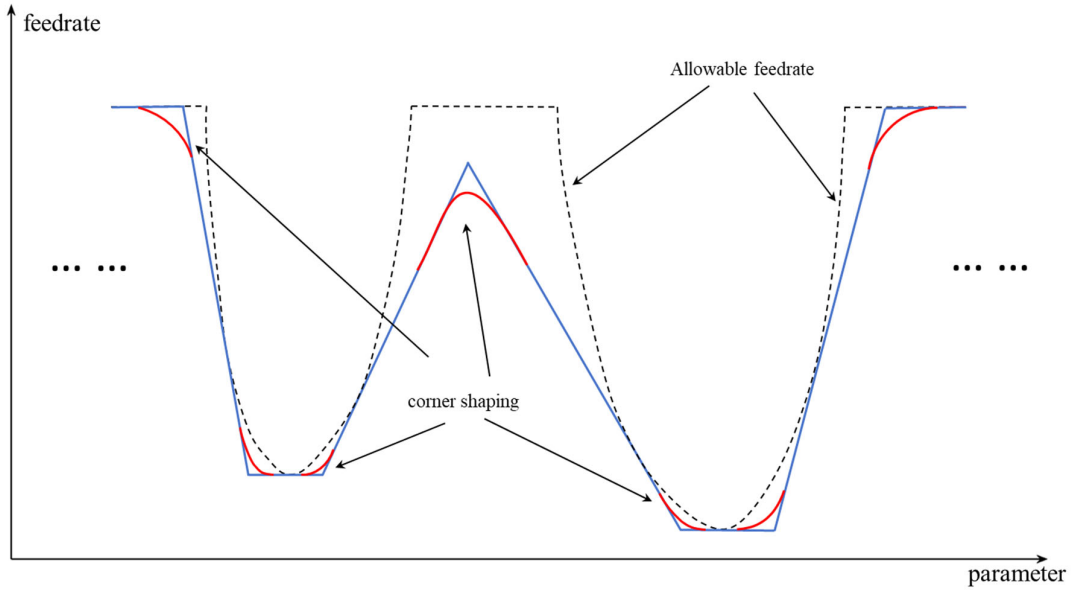


Figure 5. Example of corner shaping.

Boundary Conditions:

$$\begin{cases} V(0) = V_L \\ V'(0) = V_L' \cdot h \\ V''(0) = V_L'' \cdot h^2 \\ V(1) = V_R \\ V'(1) = V_R' \cdot h \\ V''(1) = V_R'' \cdot h \end{cases} \tag{28}$$

Substituting into Equation (27), the matrix form $A\mathbf{a} = \mathbf{b}$ can be obtained as:

$$\begin{pmatrix} 1 & 0 & 0 & 0 & 0 & 0 \\ 0 & 1 & 0 & 0 & 0 & 0 \\ 0 & 0 & 2 & 0 & 0 & 0 \\ 1 & 1 & 1 & 1 & 1 & 1 \\ 0 & 1 & 2 & 3 & 4 & 5 \\ 0 & 0 & 2 & 6 & 12 & 20 \end{pmatrix} \begin{pmatrix} a_0 \\ a_1 \\ a_2 \\ a_3 \\ a_4 \\ a_5 \end{pmatrix} = \begin{pmatrix} V_L \\ V_L' h \\ V_L'' h^2 \\ V_R \\ V_R' h \\ V_R'' h^2 \end{pmatrix} \tag{29}$$

Then, the polynomial coefficients can be solved as $\mathbf{a} = A^{-1}\mathbf{b}$.

Since $u = h\omega + u_L$, it follows that $u^n = h^n \omega^n$. Therefore, the relationship between the derivatives of the polynomial with respect to ω and with respect to u is given by:

$$\frac{d^n V}{du^n} = \frac{1}{h^n} \frac{d^n V}{d\omega^n} \tag{30}$$

From Equations (21) and (23), it can be seen that both the tangential jerk and the axis jerks are influenced by the feedrate and its derivatives. Further, combining with Equation (30), it can be deduced that, under the same polynomial coefficients, the derivative of the feedrate with respect to the parameter u decreases as the local smoothing window width h increases. Therefore, by appropriately adjusting the scale of the local smoothing window, the tangential jerk and axis jerks can be effectively reduced, enabling the generation of a feedrate profile that satisfies jerk constraints.

In summary, the specific procedure of the feedrate planning method based on curve shaping is as follows:

1. Determine the machining path and calculate the maximum allowable feedrate at each sample point under static constraints to obtain the initial feedrate profile.
2. Identify the FSRs, determine the start and end parameters of each region, the parameters of local maxima and minima, and their corresponding feedrates.
3. Identify the points within each FSR that satisfy dynamic constraints; these points are defined as feasible points.
4. At each feasible point, draw a tangent line with the slope equal to the local derivative of the feedrate. This tangent intersects with a constant feedrate line—either the programmed feedrate in non-sensitive regions or the feedrate at the local maximum of the sensitive region—at one point, and with a constant feedrate line at the local minimum of the sensitive region at another point. By traversing the entire acceleration and deceleration process in this manner, the complete feedrate profile along the path is obtained.
5. Apply corner shaping to the transition segments of the resulting complete feedrate profile to produce a final smooth feedrate curve.

4. Simulation and Experimental Validation

In this section, the proposed feedrate planning algorithm based on FPS is validated through simulations and experiments. The results confirm the feasibility of the proposed

method. The simulation platform is a personal computer equipped with an Intel Core i5-8265U 1.6 GHz processor, manufactured by Intel Corporation, Santa Clara, California, USA, and all models were developed and executed in MATLAB R2023b.

4.1. Simulation Case

4.1.1. Three-Axis Parametric Path

In this study, a WM-type NURBS toolpath with continuous curvature variation, containing both high-curvature and low-curvature regions, was designed as the test object. Its geometry and control points are shown in Figure 6. The curve is defined by the following parameters: the degree p is 3; the knot vector$\{U_i\}$ = {0,0,0,0,0.2,0.4,0.6,0.8,1,1,1,1}; the control points $\{P_i\}$ = {[0,0],[10,−12],[15,1],[17,−11],[25,12],[30,−7],[32,3],[40,−10]}; and the weight vector$\{\omega_i\}$ = {1,2,1.5,3,2.5,3.5,3.5,1}.

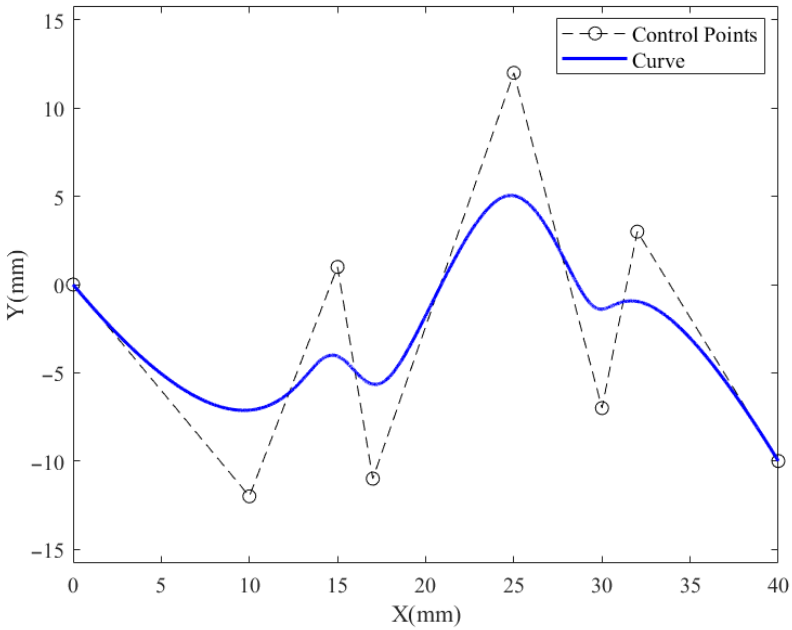


Figure 6. Geometric model of the WM curve.

To verify the applicability and stability of the proposed feedrate planning method under multiple constraints, complete simulation test conditions were designed based on machining engineering experience. These conditions include the geometric parameters of the toolpath, interpolation period, and various kinematic constraint limits. The specific parameter configuration is listed in Table 1.

Table 1. Three-axis Interpolator Parameters.

Symbol	Parameter	Value
T	Interpolation period	1 ms
$\delta_{\max}$	Chord error limitation	1 μm
v_p	Programmed maximum feedrate	70 mm/s
$a_{n,\max}$	Normal acceleration limitation	950 mm/s^2
$j_{n,\max}$	Normal jerk limitation	26,000 mm/s^3
$\hat{f}_{\lim}$	Axis feedrate limitation	100 mm/s
$\hat{A}_{\max}$	Axis acceleration limitation	1000 mm/s^2
$\hat{J}_{\max}$	Axis jerk limitation	10,000 mm/s^3

Furthermore, to demonstrate the advantages of the proposed feedrate planning algorithm, a simulation was also conducted using a constant feedrate strategy within FSRs,

and the results were compared with those of the proposed method, as shown in Figure 7. Analysis indicates that although the constant feedrate strategy can satisfy the maximum constraint limits, its planning approach within FSRs is limited, as it only uses the allowable feedrate at curvature maxima as the constant feedrate. While this method can meet the basic requirements for machining stability, it considerably reduces feedrate efficiency.

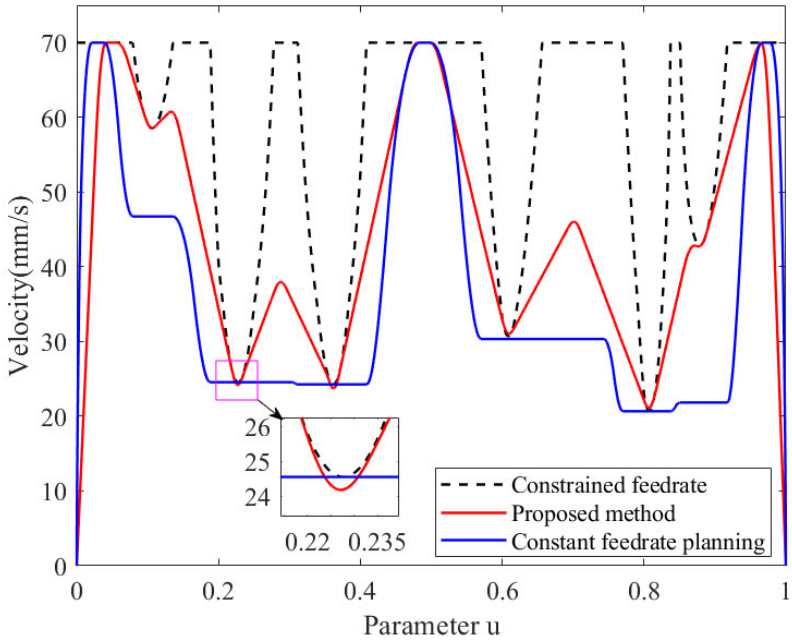


Figure 7. Comparison of two feedrate planning methods for the WM curve.

By applying the feedrate planning method proposed in this study, which is based on FPS, the resulting feedrate curve satisfies the preset kinematic constraints in both feedrate-sensitive and non-sensitive regions, without exceeding the allowable feedrate. All axis velocities are smoothly maintained within their respective limits, as shown in Figure 8. Moreover, the feedrate curve generated using the profile shaping strategy ensures that the accelerations of all drive axes remain strictly within their limits, as illustrated in Figure 9. Furthermore, by applying corner shaping to smooth the feedrate curve and adjusting the smoothing window size, the jerks of all drive axes are kept within the constraint range, as shown in Figure 10. Therefore, the proposed method can improve machining efficiency while satisfying machine axis drive constraints, effectively balancing constraint compliance and efficiency objectives. Compared with the reference algorithm, the proposed method demonstrates an average feedrate increase of 28.74% along the tool path for this case study.

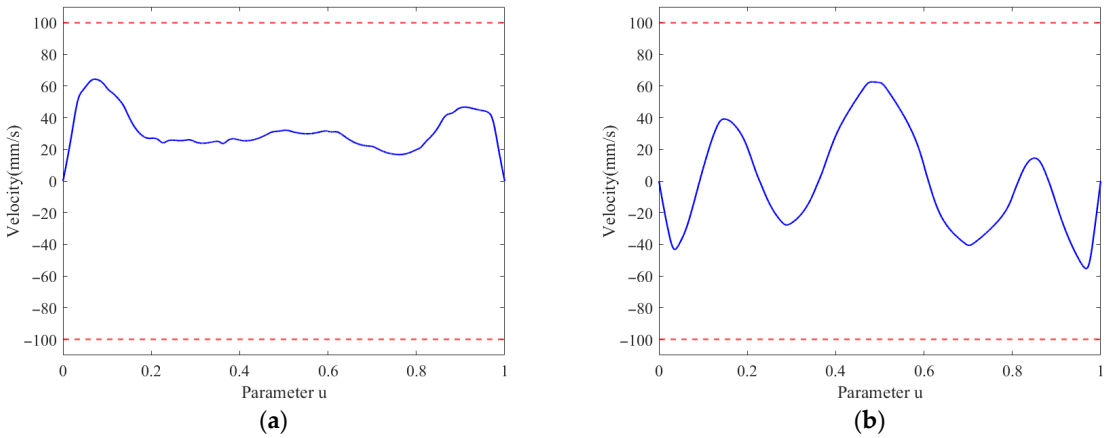


Figure 8. Axis velocity. (**a**) X-axis velocity; (**b**) Y-axis velocity.

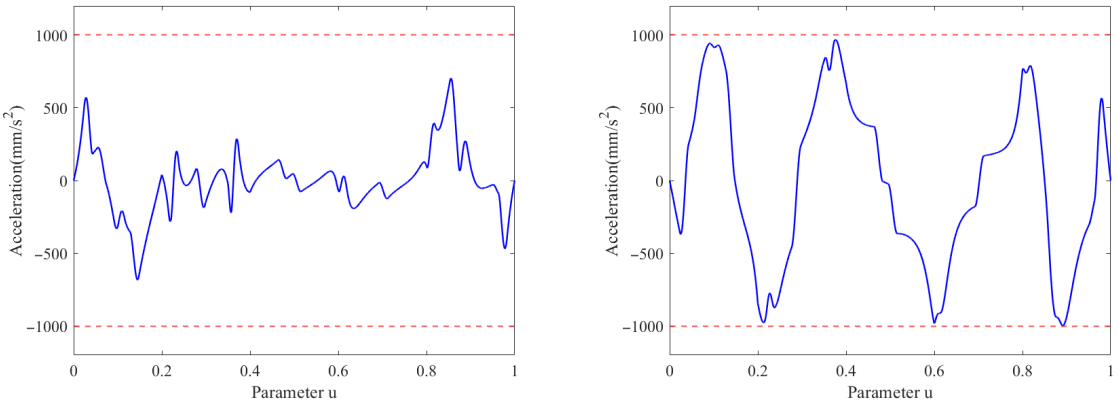


Figure 9. Axis acceleration. (**a**) X-axis acceleration; (**b**) Y-axis acceleration.

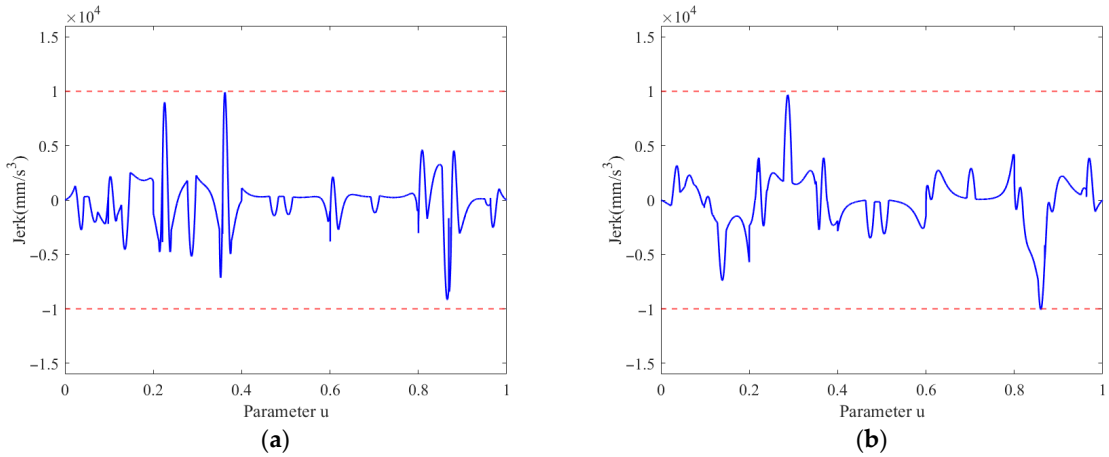


Figure 10. Axis jerk. (**a**) X-axis jerk; (**b**) Y-axis jerk.

4.1.2. Five-Axis Parametric Path

To verify that the proposed algorithm is also applicable to feedrate planning in five-axis CNC machining, a parametric path for an AC-type five-axis dual-turntable machine tool is designed for simulation to test the reliability and effectiveness of the method. Figure 11 shows the five-axis machining path represented by two NURBS curves. Except for the control points shown in the figure, the knot vectors are uniformly distributed and all weights are set to 1. Table 2 lists the relevant parameters used in the simulation experiments.

Table 2. Five-axis Interpolator Parameters.

Symbol	Parameter	Value
T	Interpolation period	1 ms
$\delta_{\max}$	Chord error limitation	1 μm
v_p	Programmed maximum feedrate	50 mm/s
$a_{n,\max}$	Normal acceleration limitation	800 mm/s^2
$j_{n,\max}$	Normal jerk limitation	8000 mm/s^3
$\hat{f}_{l,\lim}$	Linear axis feedrate limitation	100 mm/s
$\hat{f}_{r,\lim}$	Rotation axis feedrate limitation	30°/s
$\hat{A}_{l,\max}$	Linear axis acceleration limitation	300 mm/s^2
$\hat{A}_{r,\max}$	Rotation axis acceleration limitation	100°/s^2
$\hat{J}_{l,\max}$	Linear axis jerk limitation	3000 mm/s^3
$\hat{J}_{r,\max}$	Rotation axis jerk limitation	700°/s^3

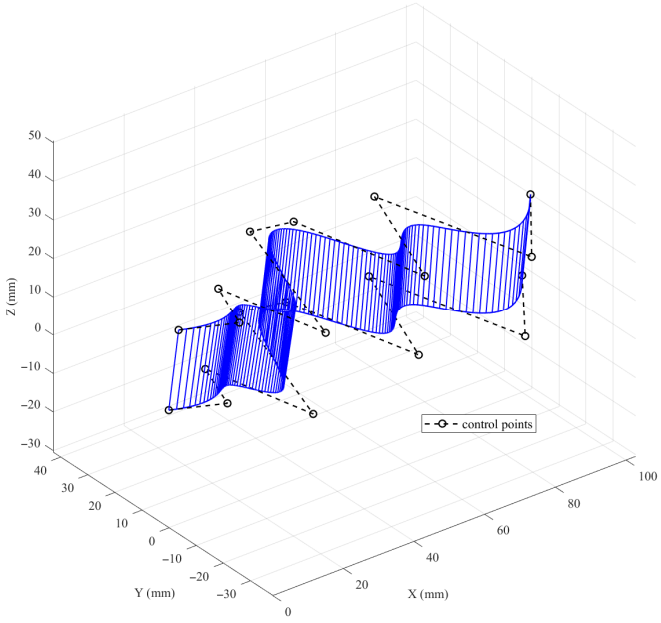


Figure 11. Five-axis parametric path.

Based on the parameters listed in Table 2 and the parametric path shown in Figure 11, the proposed FPS algorithm was applied to plan the feedrate along the double NURBS curves. The planning results are shown in Figure 12, where the blue dashed line represents the allowable feedrate curve under static constraints, and the red solid line represents the actual feedrate curve planned using the FPS algorithm. It can be observed that the planned feedrate remains strictly below the static constraint curve, with no violations. Moreover, smooth transitions between adjacent FSRs are achieved through FPS. These results indicate that the proposed method ensures motion smoothness and constraint feasibility while also maintaining high machining efficiency.

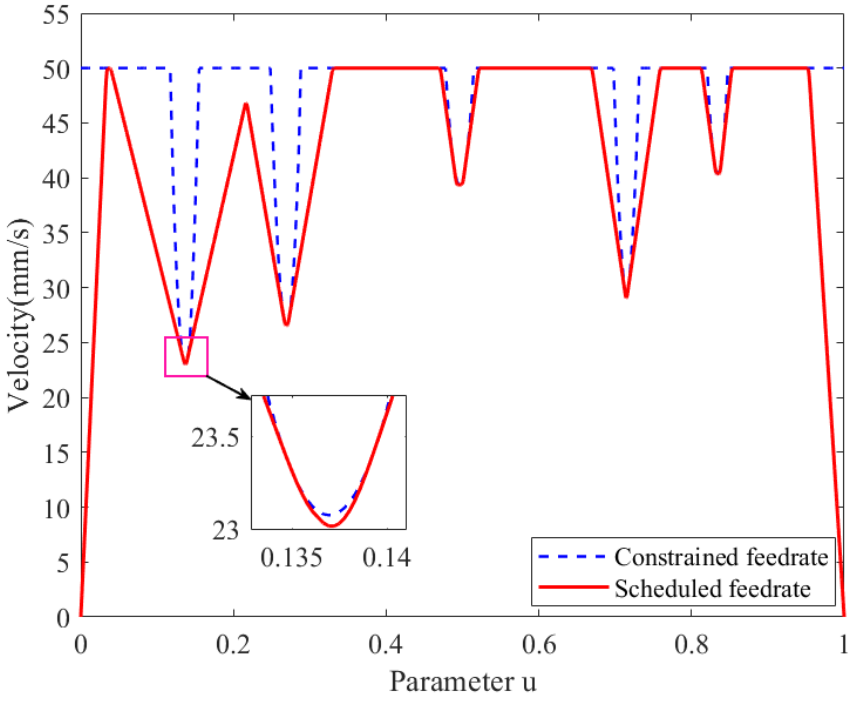
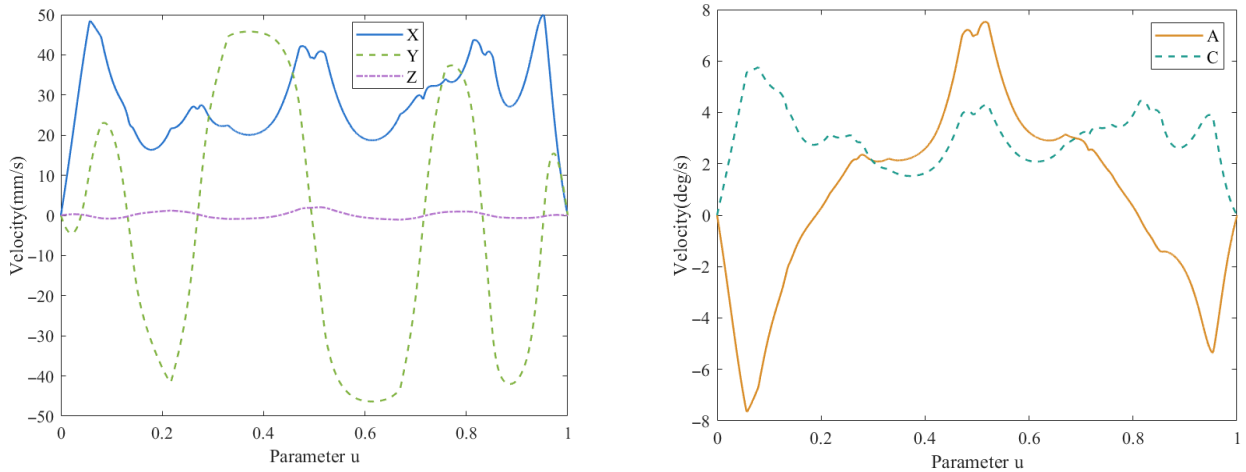


Figure 12. The scheduled federate for five-axis parametric path.

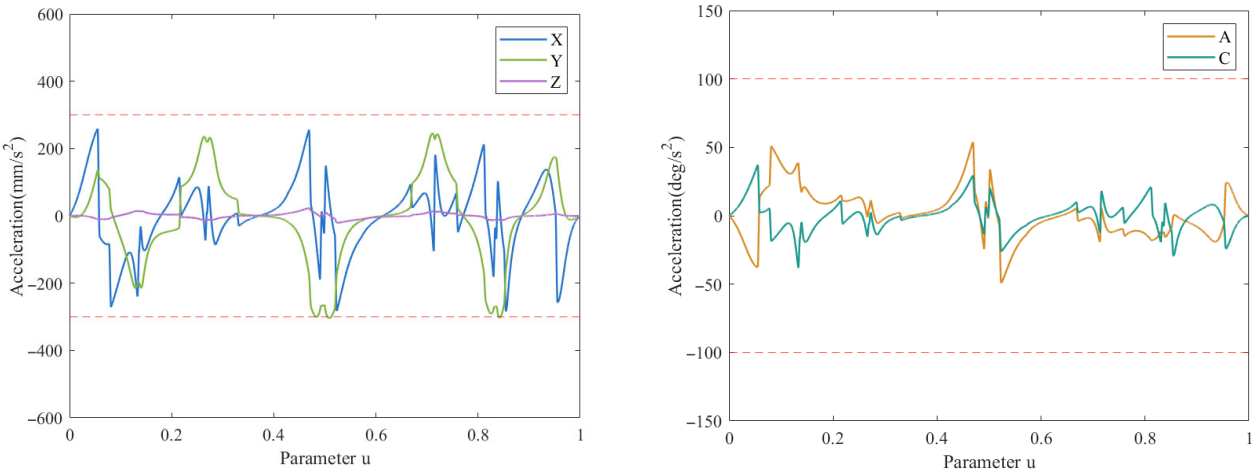
Figure 13 shows the axis-specific velocity curves after applying the FPS algorithm, with the linear axis velocities on the left and the rotary axis velocities on the right. As seen in the figure, the axis velocity curves are well-smoothed, avoiding abrupt changes and ensuring machining quality. Both the linear and rotary axis velocities are strictly maintained within their respective constraint limits.



(**a**) (**b**)

Figure 13. The axis velocity of five-axis machining. (**a**) Linear axis velocity; (**b**) Rotary axis velocity.

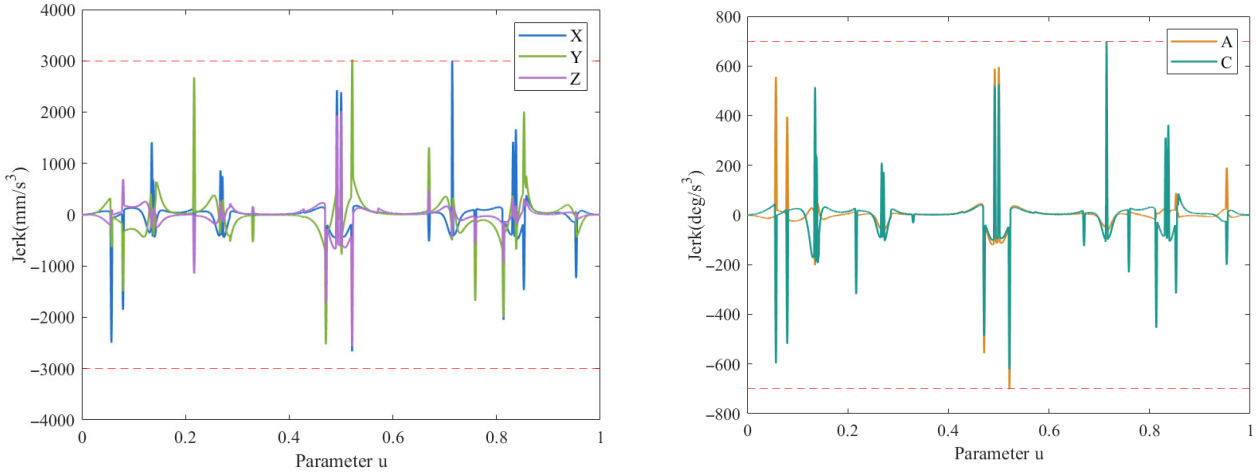
Figure 14 shows the axis-specific acceleration curves after applying the FPS algorithm, with linear axis accelerations on the left and rotary axis accelerations on the right. It can be seen that the accelerations of both the linear and rotary axes are strictly maintained within their respective constraint limits.



(**a**) (**b**)

Figure 14. The axis acceleration of five-axis machining. (**a**) Linear axis acceleration; (**b**) Rotary axis acceleration.

Figure 15 shows the axis-specific jerk (rate of change in acceleration) curves after applying the FPS algorithm, with the linear axis jerks on the left and the rotary axis jerks on the right. As observed, the jerks of both the linear and rotary axes are strictly maintained within their respective constraint limits.



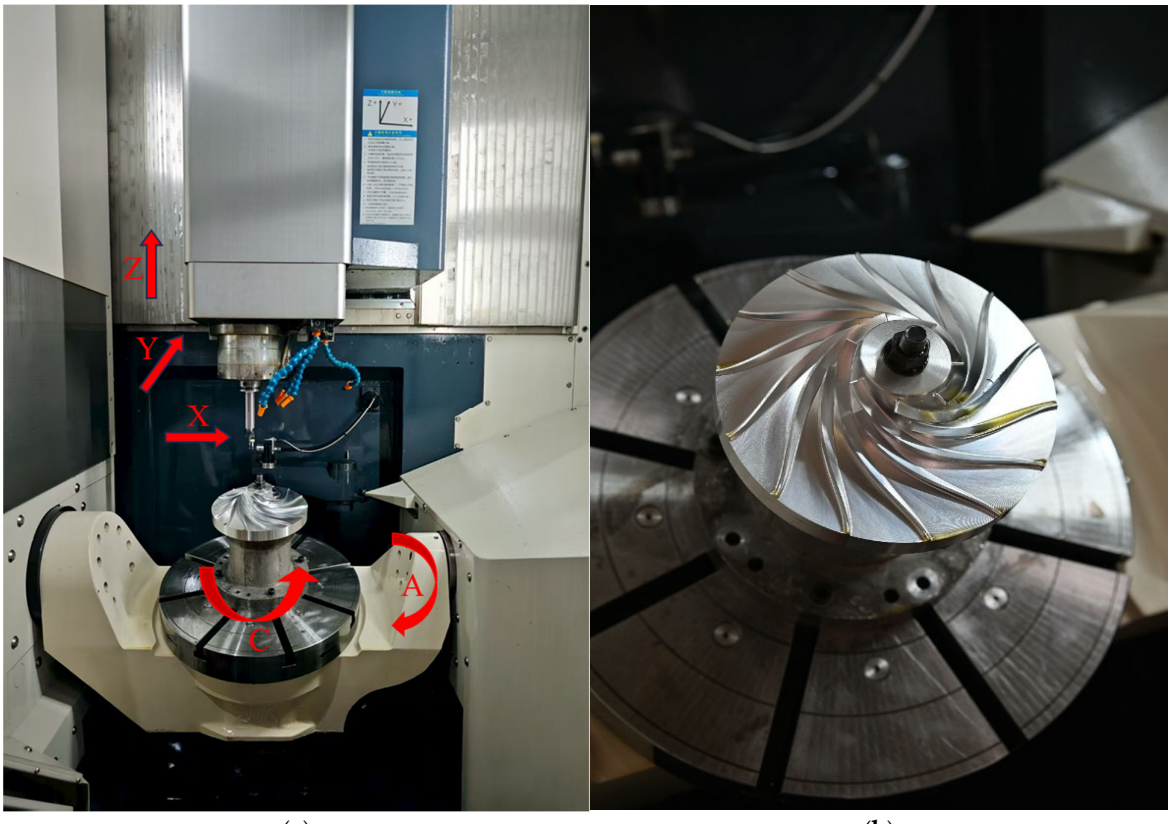
(**a**) (**b**)

Figure 15. The axis jerk of five-axis machining. (**a**) Linear axis jerk; (**b**) Rotary axis jerk.

In summary, the kinematic parameters of all axes were well constrained within the limits specified in Table 2, demonstrating the effectiveness of the proposed algorithm in respecting the drive capabilities of the machine axes.

4.2. Five-Axis Machining Experimental Validation

To evaluate the performance of the proposed feedrate planning algorithm in a practical machining scenario, experiments were conducted on a five-axis dual-turntable CNC machine. The experimental setup, including the machine and the workpiece used for testing, is shown in Figure 16.



(**a**) (**b**)

Figure 16. Experimental setup and impeller workpiece. (**a**) Five-axis dual-turntable machine; (**b**) Impeller workpiece.

The five-axis machine tool used is equipped with two rotary axes (A-axis and C-axis) mounted on a dual rotary table structure, as shown in Figure 16a. This configuration allows for five-axis simultaneous motion and provides high flexibility for the machining of complex free-form surfaces. Due to its high positioning accuracy and motion performance, this setup is widely used in the manufacturing of impellers and other multi-axis components. In the machining experiments, the programmed feedrate was 1000 mm/min. The linear axis velocity limit was 15,000 mm/min, and the rotary axis velocity limit was 5000°/min.

The test workpiece is an impeller, as shown in Figure 16b. It is a typical complex surface part characterized by twisted blades, significant curvature variations, and substantial changes in tool orientation during the machining process. These geometric features impose stringent requirements on feedrate planning and axis coordination. Therefore, the impeller serves as an ideal benchmark part for validating the effectiveness and robustness of the proposed feedrate planning algorithm. The material of the test workpiece is aluminum alloy, which is commonly used in aerospace and high-speed machining applications.

The proposed algorithm was applied to the machining of impeller blades, and the results were compared with those obtained using the original G-code. The blades machined with the proposed method exhibited superior surface quality, characterized by an absence of chatter marks, scratches, or other surface defects. In contrast, the surfaces produced using the original G-code showed noticeable waviness and surface irregularities, as shown in Figure 17.

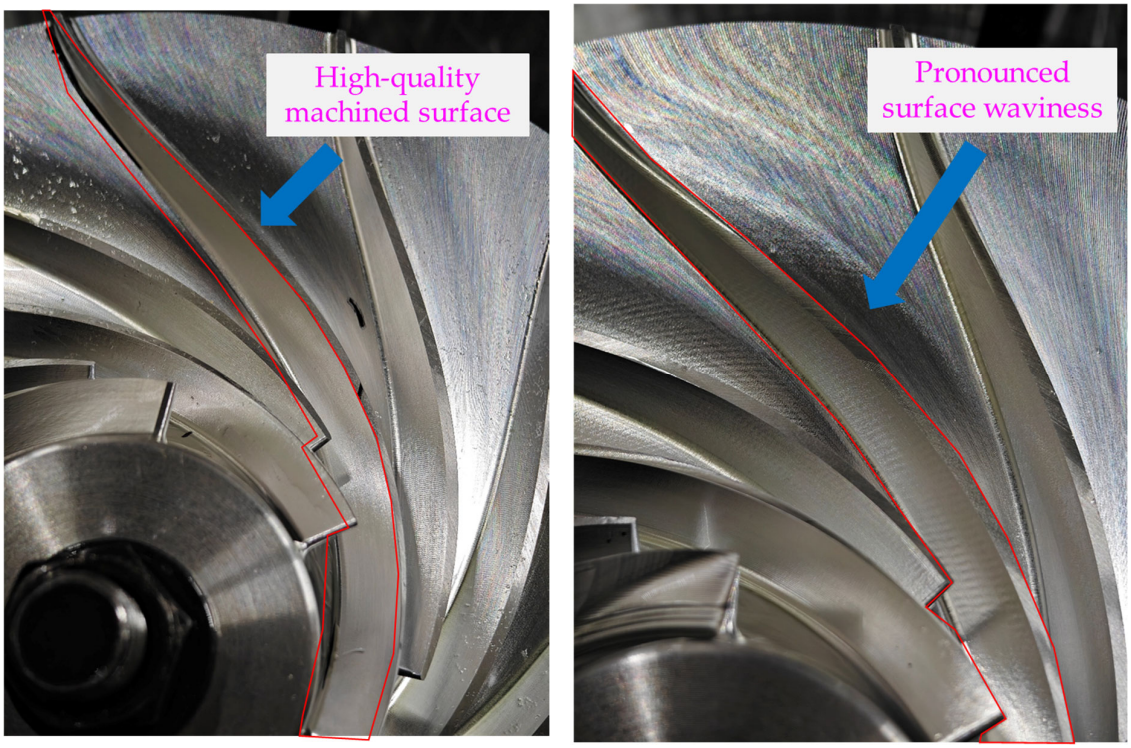


Figure 17. Comparison of the actual machining results. (**a**) Machining results of the proposed method; (**b**) Machining results with the original G-code.

In addition, this study introduces the concept of feedrate fluctuation to evaluate machining stability from the perspective of feedrate planning. The feedrate fluctuation is calculated as follows [20]:

$$\varepsilon_{i+1} = \left| \frac{\frac{\|p(u_{i+1}) - p(u_i)\|}{T} - v_{i+1}}{v_{i+1}} \right| \times 100\% \quad (31)$$

For the proposed feedrate planning method, the maximum feedrate fluctuation is 2.25×10^{-14}%, and the average feedrate fluctuation is 5.42×10^{-15}%. In comparison, for the original G-code machining, the maximum feedrate fluctuation is 1.95×10^{-6}%, and the average feedrate fluctuation is 6.3×10^{-7}%. These results indicate that the proposed feedrate planning method significantly reduces feedrate fluctuations, leading to smoother variations in feedrate during machining and lower dynamic excitation, thereby improving machining stability.

Furthermore, the application of the proposed feedrate planning strategy resulted in a significant improvement in machining efficiency, with an observed increase of approximately 10% compared to conventional processing. These results demonstrate that the proposed algorithm not only ensures high-quality surface finishes but also enhances the machining performance.

5. Conclusions

This paper proposes an adaptive feedrate planning method for parametric paths based on curve shaping, aiming to achieve maximum feedrate performance along toolpaths in high-speed CNC machining while satisfying both the geometric constraints of the parametric path and the drive constraints of machine axes. The main research contributions are summarized as follows:

(1) Based on the derived geometric characteristics of the toolpath, the kinematic properties of the machine drive axes, and the analytical relationships between trajectory curve parameters and feedrate profile parameters, a theoretical constraint model for the proposed method was established.

(2) A complete feedrate profile is generated using a curve shaping strategy, achieving maximum feedrate along the parametric path while satisfying geometric, normal, and tangential constraints as well as machine axis drive limitations.

(3) The feedrate curve is corner-shaped using a local smoothing approach to produce a smooth feedrate profile that satisfies the jerk limits of all drive axes.

(4) The effectiveness of the proposed method was validated through simulations and experiments. Compared with existing approaches, the proposed algorithm achieves an average feedrate increase of 28.74% along the tool path for the WM-type parametric path, and approximately 10% higher machining efficiency in the actual machining of an impeller blade. The results demonstrate that the proposed method can significantly enhance machining efficiency while strictly satisfying multiple constraints, thereby achieving an effective balance between constraint compliance and productivity.

Despite these advantages, the proposed method has certain limitations. Its performance depends on the accuracy of the parametric path representation and the availability of reliable machine axis constraint information. In addition, for extremely complex toolpaths with frequent changes in curvature and tool orientation, the computational cost of constraint evaluation and feedrate shaping may increase. These aspects will be further investigated in future work.

From an industrial perspective, the proposed feedrate planning method is suitable for high-speed and high-quality five-axis machining of complex free-form surfaces, such as impellers. The method can be integrated into offline CNC feedrate planning modules, providing a practical solution for improving machining efficiency while ensuring strict compliance with machine axis constraints.

Author Contributions: Conceptualization, S.Z. and Y.L.; methodology, S.Z. and Y.L.; software, S.Z. and Q.M.; validation, S.Z., Q.M., H.Y. and D.W.; formal analysis, S.Z. and Q.M.; investigation, S.Z., D.W. and J.L.; resources, W.H., D.W. and H.Y.; data curation, S.Z., Q.M. and Y.W.; writing—original draft preparation, S.Z.; writing—review and editing, W.H., Q.M., Y.L. and J.C.; visualization, S.Z., J.C. and J.L.; supervision, W.H. and D.W.; project administration, L.W., D.W. and W.H.; funding acquisition, L.W., D.W. and W.H. All authors have read and agreed to the published version of the manuscript.

Funding: This research was funded by the National Natural Science Foundation of China, grant number 52375448.

Data Availability Statement: The original contributions presented in this study are included in the article. Further inquiries can be directed to the corresponding author.

Conflicts of Interest: The authors declare no conflicts of interest.

Abbreviations

The following abbreviations are used in this manuscript:

CNC	Computer numerical control
CAD	Computer-aided design
CAM	Computer-aided manufacturing
CAE	Computer-aided engineering
NURBS	Non-uniform rational B-splines
FSR	Feedrate-sensitive region
PMR	Points of minimum curvature radius
FPS	Feedrate profile shaping

References

1. Sencer, B.; Dumanli, A.; Yamada, Y. Spline interpolation with optimal frequency spectrum for vibration avoidance. *CIRP Ann.* **2018**, *67*, 377–380. [CrossRef]
2. Ji, S.; Lei, L.; Zhao, J.; Lu, X.; Gao, H. An adaptive real-time NURBS curve interpolation for 4-axis polishing machine tool. *Robot. Comput. Integr. Manuf.* **2021**, *67*, 102025. [CrossRef]
3. Hu, Y.; Jiang, X.; Huo, G.; Su, C.; Zhou, S.; Wang, B.; Li, H.; Zheng, Z. A novel feed rate scheduling method with acc-jerk-continuity and round-off error elimination for non-uniform rational B-spline interpolation. *J. Comput. Des. Eng.* **2023**, *10*, 294–317. [CrossRef]
4. Liu, Q.; Hu, J.; Li, P.; Liu, S.; Huang, G.; Zhang, X.; Wei, Y.; Hao, T.; Shen, J. A NURBS interpolation method using circular arc mapping and improved S-shaped acc/dec algorithm based on filter processing. *J. Manuf. Process.* **2025**, *154*, 422–443. [CrossRef]
5. Wang, L.; Li, Y.; Yang, H.; Li, J. Surface-centric toolpath optimization via cutter location surface reconstruction for addressing neighboring inconsistency in CNC machining. *J. Manuf. Process.* **2025**, *150*, 933–948. [CrossRef]
6. Jiang, Y.; Liu, K.; Huang, J.; Zhao, D.; Gao, P.; Li, M.; Liu, H.; Wang, Y. Research on feedrate intelligent control method for machining efficiency. *Mech. Syst. Signal Process.* **2025**, *236*, 113037. [CrossRef]
7. Wang, L.; Zhang, J.; Li, W.; Wang, Y.; Zhou, Y. Research on feedrate scheduling method for NURBS toolpath interpolation in high-speed CNC machining. *Int. J. Adv. Manuf. Technol.* **2025**, *138*, 3293–3313. [CrossRef]
8. Sun, Y.; Zhao, Y.; Bao, Y.; Guo, D. A novel adaptive-feedrate interpolation method for NURBS tool path with drive constraints. *Int. J. Mach. Tools Manuf.* **2014**, *77*, 74–81. [CrossRef]
9. Sun, Y.; Jia, J.; Xu, J.; Chen, M.; Niu, J. Path, feedrate and trajectory planning for free-form surface machining: A state-of-the-art review. *Chin. J. Aeronaut.* **2022**, *35*, 12–29. [CrossRef]
10. Zhao, J.; Lou, Y.; Shi, R.; Zhang, Z. A Time-Optimal Velocity Planning Algorithm with Machining Precision Constraints for CNC System. In Proceedings of the 2019 IEEE 9th Annual International Conference on CYBER Technology in Automation, Control, and Intelligent Systems (CYBER), Suzhou, China, 29 July–2 August 2019; pp. 1348–1353. [CrossRef]
11. Guo, P.; Wu, Y.; Yang, G.; Shen, Z.; Zhang, H.; Zhang, P.; Lou, F.; Li, H. A Feedrate Planning Method for the NURBS Curve in CNC Machining Based on the Critical Constraint Curve. *Appl. Sci.* **2021**, *11*, 4959. [CrossRef]
12. Zhang, K.; Yuan, C.-M.; Gao, X.-S.; Li, H. A greedy algorithm for feedrate planning of CNC machines along curved tool paths with confined jerk. *Robot. Comput. Integr. Manuf.* **2012**, *28*, 472–483. [CrossRef]
13. Beudaert, X.; Pechard, P.-Y.; Tournier, C. 5-Axis tool path smoothing based on drive constraints. *Int. J. Mach. Tools Manuf.* **2011**, *51*, 958–965. [CrossRef]

14. Sang, Y.; Yao, C.; Lv, Y.; He, G. An improved feedrate scheduling method for NURBS interpolation in five-axis machining. *Precis. Eng.* **2020**, *64*, 70–90. [CrossRef]
15. Ma, H.-Y.; Yuan, C.-M.; Shen, L.-Y.; Gao, X.-S. Optimal feedrate planning on a five-axis parametric tool path with global geometric and kinematic constraints. *J. Comput. Des. Eng.* **2022**, *9*, 2355–2374. [CrossRef]
16. Tang, P.-Y.; Lin, M.-T.; Tsai, M.-S. Real-time master-based feedrate scheduling with kinematic constraints for five-axis machining. *Int. J. Adv. Manuf. Technol.* **2022**, *123*, 493–510. [CrossRef]
17. Huang, Y.; Tang, Q.; Wei, W.; Wang, Y.; Hu, T.; Huang, W. Speed partition optimization algorithm in five-axis machining under jerk constraints. *Int. J. Adv. Manuf. Technol.* **2025**, *140*, 721–742. [CrossRef]
18. Huang, J.; Zhu, L.-M. Feedrate scheduling for interpolation of parametric tool path using the sine series representation of jerk profile. *Proc. Inst. Mech. Eng. Part B J. Eng. Manuf.* **2016**, *231*, 2359–2371. [CrossRef]
19. Wang, T.-Y.; Zhang, Y.-B.; Dong, J.-C.; Ke, R.-J.; Ding, Y.-Y. NURBS Interpolator with Adaptive Smooth Feedrate Scheduling and Minimal Feedrate Fluctuation. *Int. J. Precis. Eng. Manuf.* **2019**, *21*, 273–290. [CrossRef]
20. Jia, Z.; Song, D.; Ma, J.; Hu, G.; Su, W. A NURBS interpolator with constant speed at feedrate-sensitive regions under drive and contour-error constraints. *Int. J. Mach. Tools Manuf.* **2017**, *116*, 1–17. [CrossRef]
21. Ma, J.; Jia, Z.; Qin, F.; Song, D.; Jiang, W.; Chen, S. A Five-Axis Dual NURBS Interpolator with Constant Speed at Feedrate-Sensitive Regions Under Axial Drive Constraints. *J. Manuf. Sci. Eng.* **2019**, *141*, 061002. [CrossRef]
22. Nie, M.; Wan, Y.; Zhou, A. Real-Time NURBS Interpolation under Multiple Constraints. *Comput. Intell. Neurosci.* **2022**, *2022*, 7492762. [CrossRef]

Disclaimer/Publisher's Note: The statements, opinions and data contained in all publications are solely those of the individual author(s) and contributor(s) and not of MDPI and/or the editor(s). MDPI and/or the editor(s) disclaim responsibility for any injury to people or property resulting from any ideas, methods, instructions or products referred to in the content.